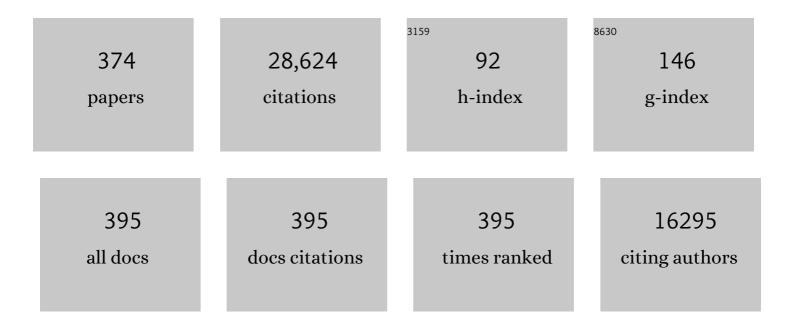
List of Publications by Year in descending order

Source: https://exaly.com/author-pdf/7832035/publications.pdf Version: 2024-02-01



LVNDON EMSLEY

#	Article	IF	CITATIONS
1	Multiâ€Length Scale Structure of 2D/3D Dion–Jacobson Hybrid Perovskites Based on an Aromatic Diammonium Spacer. Small, 2022, 18, e2104287.	10.0	10
2	Hyperpolarized Solution-State NMR Spectroscopy with Optically Polarized Crystals. Journal of the American Chemical Society, 2022, 144, 2511-2519.	13.7	25
3	Colloidal-ALD-Grown Hybrid Shells Nucleate via a Ligand–Precursor Complex. Journal of the American Chemical Society, 2022, 144, 3998-4008.	13.7	12
4	Efficient and Stable Large Bandgap MAPbBr <sub>3</sub> Perovskite Solar Cell Attaining an Open Circuit Voltage of 1.65 V. ACS Energy Letters, 2022, 7, 1112-1119.	17.4	21
5	Spatial Distribution of Functional Groups in Cellulose Ethers by DNP-Enhanced Solid-State NMR Spectroscopy. Macromolecules, 2022, 55, 2952-2958.	4.8	11
6	In-Cell Quantification of Drugs by Magic-Angle Spinning Dynamic Nuclear Polarization NMR. Journal of the American Chemical Society, 2022, 144, 6734-6741.	13.7	13
7	<i>De Novo</i> Crystal Structure Determination from Machine Learned Chemical Shifts. Journal of the American Chemical Society, 2022, 144, 7215-7223.	13.7	14
8	<sup>1</sup> H Detected Relayed Dynamic Nuclear Polarization. Journal of Physical Chemistry C, 2022, 126, 7564-7570.	3.1	7
9	Design Principles for the Development of Gd(III) Polarizing Agents for Magic Angle Spinning Dynamic Nuclear Polarization. Journal of Physical Chemistry C, 2022, 126, 11310-11317.	3.1	10
10	Hyperpolarization transfer pathways in inorganic materials. Journal of Magnetic Resonance, 2021, 323, 106888.	2.1	6
11	Scaling analyses for hyperpolarization transfer across a spin-diffusion barrier and into bulk solid media. Physical Chemistry Chemical Physics, 2021, 23, 1006-1020.	2.8	35
12	High Sensitivity Detection of a Solubility Limiting Surface Transformation of Drug Particles by DNP SENS. Journal of Pharmaceutical Sciences, 2021, 110, 2452-2456.	3.3	3
13	Solid-state NMR spectroscopy. Nature Reviews Methods Primers, 2021, 1, .	21.2	196
14	Similarities and Differences among Protein Dynamics Studied by Variable Temperature Nuclear Magnetic Resonance Relaxation. Journal of Physical Chemistry B, 2021, 125, 2212-2221.	2.6	6
15	Pseudo-halide anion engineering for α-FAPbI3 perovskite solar cells. Nature, 2021, 592, 381-385.	27.8	2,095
16	The Atomic-Level Structure of Cementitious Calcium Aluminate Silicate Hydrate Determined by NMR. Chimia, 2021, 75, 272-275.	0.6	1
17	Iron incorporation in synthetic precipitated calcium silicate hydrates. Cement and Concrete Research, 2021, 142, 106365.	11.0	14
18	Benzylammoniumâ€Mediated Formamidinium Lead Iodide Perovskite Phase Stabilization for Photovoltaics. Advanced Functional Materials, 2021, 31, 2101163.	14.9	28

#	Article	IF	CITATIONS
19	Structure determination of an amorphous drug through large-scale NMR predictions. Nature Communications, 2021, 12, 2964.	12.8	35
20	Two-step immobilization of metronidazole prodrug on TEMPO cellulose nanofibrils through thiol-yne click chemistry for in situ controlled release. Carbohydrate Polymers, 2021, 262, 117952.	10.2	9
21	Advanced characterization of regioselectively substituted methylcellulose model compounds by DNP enhanced solid-state NMR spectroscopy. Carbohydrate Polymers, 2021, 262, 117944.	10.2	18
22	Multimodal host–guest complexation for efficient and stable perovskite photovoltaics. Nature Communications, 2021, 12, 3383.	12.8	72
23	Pure Isotropic Proton Solid State NMR. Journal of the American Chemical Society, 2021, 143, 9834-9841.	13.7	15
24	Theory and simulations of homonuclear three-spin systems in rotating solids. Journal of Chemical Physics, 2021, 155, 084201.	3.0	10
25	Endogenous <sup>17</sup> 0 Dynamic Nuclear Polarization of Gd-Doped CeO <sub>2</sub> from 100 to 370 K. Journal of Physical Chemistry C, 2021, 125, 18799-18809.	3.1	18
26	Naphthalenediimide/Formamidinium-Based Low-Dimensional Perovskites. Chemistry of Materials, 2021, 33, 6412-6420.	6.7	16
27	NMR spectroscopy probes microstructure, dynamics and doping of metal halide perovskites. Nature Reviews Chemistry, 2021, 5, 624-645.	30.2	73
28	Quantification of magic angle spinning dynamic nuclear polarization NMR spectra. Journal of Magnetic Resonance, 2021, 329, 107030.	2.1	6
29	Nanoscale Phase Segregation in Supramolecular π-Templating for Hybrid Perovskite Photovoltaics from NMR Crystallography. Journal of the American Chemical Society, 2021, 143, 1529-1538.	13.7	55
30	A Magic Angle Spinning Activated <sup>17</sup> O DNP Raser. Journal of Physical Chemistry Letters, 2021, 12, 345-349.	4.6	23
31	Unravelling the Behavior of Dion–Jacobson Layered Hybrid Perovskites in Humid Environments. ACS Energy Letters, 2021, 6, 337-344.	17.4	44
32	Bayesian probabilistic assignment of chemical shifts in organic solids. Science Advances, 2021, 7, eabk2341.	10.3	13
33	Cellulose phosphorylation comparison and analysis of phosphorate position on cellulose fibers. Carbohydrate Polymers, 2020, 229, 115294.	10.2	61
34	Supramolecular Modulation of Hybrid Perovskite Solar Cells via Bifunctional Halogen Bonding Revealed by Two-Dimensional <sup>19</sup> F Solid-State NMR Spectroscopy. Journal of the American Chemical Society, 2020, 142, 1645-1654.	13.7	69
35	Intermediate Phase Enhances Inorganic Perovskite and Metal Oxide Interface for Efficient Photovoltaics. Joule, 2020, 4, 222-234.	24.0	88
36	Structural and DNA binding properties of mycobacterial integration host factor mIHF. Journal of Structural Biology, 2020, 209, 107434.	2.8	3

#	Article	IF	CITATIONS
37	Guanine‧tabilized Formamidinium Lead Iodide Perovskites. Angewandte Chemie - International Edition, 2020, 59, 4691-4697.	13.8	61
38	Guanineâ€6tabilized Formamidinium Lead Iodide Perovskites. Angewandte Chemie, 2020, 132, 4721-4727.	2.0	0
39	Fast remote correlation experiments for 1H homonuclear decoupling in solids. Journal of Magnetic Resonance, 2020, 321, 106856.	2.1	8
40	Picometer Resolution Structure of the Coordination Sphere in the Metal-Binding Site in a Metalloprotein by NMR. Journal of the American Chemical Society, 2020, 142, 16757-16765.	13.7	33
41	Sensitivity Enhancements in Lithium Titanates by Incipient Wetness Impregnation DNP NMR. Journal of Physical Chemistry C, 2020, 124, 16524-16528.	3.1	13
42	Dynamic Nuclear Polarization Enhancement of 200 at 21.15 T Enabled by 65 kHz Magic Angle Spinning. Journal of Physical Chemistry Letters, 2020, 11, 8386-8391.	4.6	66
43	Open and Closed Radicals: Local Geometry around Unpaired Electrons Governs Magic-Angle Spinning Dynamic Nuclear Polarization Performance. Journal of the American Chemical Society, 2020, 142, 16587-16599.	13.7	42
44	<sup>113</sup> Cd Solid-State NMR at 21.1 T Reveals the Local Structure and Passivation Mechanism of Cadmium in Hybrid and All-Inorganic Halide Perovskites. ACS Energy Letters, 2020, 5, 2964-2971.	17.4	20
45	Multimodal Response to Copper Binding in Superoxide Dismutase Dynamics. Journal of the American Chemical Society, 2020, 142, 19660-19667.	13.7	15
46	Crown Ether Modulation Enables over 23% Efficient Formamidinium-Based Perovskite Solar Cells. Journal of the American Chemical Society, 2020, 142, 19980-19991.	13.7	145
47	The Atomic-Level Structure of Cementitious Calcium Aluminate Silicate Hydrate. Journal of the American Chemical Society, 2020, 142, 11060-11071.	13.7	107
48	Local Structure and Dynamics in Methylammonium, Formamidinium, and Cesium Tin(II) Mixed-Halide Perovskites from <sup>119</sup> Sn Solid-State NMR. Journal of the American Chemical Society, 2020, 142, 7813-7826.	13.7	66
49	Enhanced Intersystem Crossing and Transient Electron Spin Polarization in a Photoexcited Pentacene–Trityl Radical. Journal of Physical Chemistry A, 2020, 124, 6068-6075.	2.5	19
50	Homonuclear Decoupling in 1 Hâ€NMR of Solids by Remote Correlation. Angewandte Chemie, 2020, 132, 6294-6297.	2.0	3
51	Intermediate Phase Enhances Inorganic Perovskite and Metal Oxide Interface for Efficient Photovoltaics. Joule, 2020, 4, 507-508.	24.0	4
52	Atomistic Origins of the Limited Phase Stability of Cs <sup>+</sup> -Rich FA <sub><i>x</i></sub> Cs <sub>(1–<i>x</i>)</sub> PbI <sub>3</sub> Mixtures. Chemistry of Materials, 2020, 32, 2605-2614.	6.7	24
53	Colloidal-ALD-Grown Core/Shell CdSe/CdS Nanoplatelets as Seen by DNP Enhanced PASS–PIETA NMR Spectroscopy. Nano Letters, 2020, 20, 3003-3018.	9.1	24
54	Homonuclear Decoupling in <sup>1</sup> Hâ€NMR of Solids by Remote Correlation. Angewandte Chemie - International Edition, 2020, 59, 6235-6238.	13.8	22

#	Article	IF	CITATIONS
55	TinyPols: a family of water-soluble binitroxides tailored for dynamic nuclear polarization enhanced NMR spectroscopy at 18.8 and 21.1 T. Chemical Science, 2020, 11, 2810-2818.	7.4	72
56	Vapor-assisted deposition of highly efficient, stable black-phase FAPbI <sub>3</sub> perovskite solar cells. Science, 2020, 370, .	12.6	530
57	Measurement of Proton Spin Diffusivity in Hydrated Cementitious Solids. Journal of Physical Chemistry Letters, 2019, 10, 5064-5069.	4.6	4
58	Atomic-level passivation mechanism of ammonium salts enabling highly efficient perovskite solar cells. Nature Communications, 2019, 10, 3008.	12.8	268
59	Line narrowing in 1H NMR of powdered organic solids with TOP-CT-MAS experiments at ultra-fast MAS. Journal of Magnetic Resonance, 2019, 305, 131-137.	2.1	13
60	Atomic-Level Microstructure of Efficient Formamidinium-Based Perovskite Solar Cells Stabilized by 5-Ammonium Valeric Acid Iodide Revealed by Multinuclear and Two-Dimensional Solid-State NMR. Journal of the American Chemical Society, 2019, 141, 17659-17669.	13.7	104
61	Ba-induced phase segregation and band gap reduction in mixed-halide inorganic perovskite solar cells. Nature Communications, 2019, 10, 4686.	12.8	105
62	High-resolution 1H NMR of powdered solids by homonuclear dipolar decoupling. Journal of Magnetic Resonance, 2019, 309, 106598.	2.1	22
63	Chemical exchange at the ferroelectric phase transition of lead germanate revealed by solid state <sup>207</sup> Pb nuclear magnetic resonance. Physical Chemistry Chemical Physics, 2019, 21, 1100-1109.	2.8	11
64	Maximizing nuclear hyperpolarization in pulse cooling under MAS. Journal of Magnetic Resonance, 2019, 300, 142-148.	2.1	16
65	A Factor Two Improvement in High-Field Dynamic Nuclear Polarization from Gd(III) Complexes by Design. Journal of the American Chemical Society, 2019, 141, 8746-8751.	13.7	28
66	Dynamic Nuclear Polarization Magic-Angle Spinning Nuclear Magnetic Resonance Combined with Molecular Dynamics Simulations Permits Detection of Order and Disorder in Viral Assemblies. Journal of Physical Chemistry B, 2019, 123, 5048-5058.	2.6	31
67	19 F Magic Angle Spinning Dynamic Nuclear Polarization Enhanced NMR Spectroscopy. Angewandte Chemie, 2019, 131, 7327-7331.	2.0	2
68	Structural description of surfaces and interfaces in biominerals by DNP SENS. Solid State Nuclear Magnetic Resonance, 2019, 102, 2-11.	2.3	25
69	Rapid Structure Determination of Molecular Solids Using Chemical Shifts Directed by Unambiguous Prior Constraints. Journal of the American Chemical Society, 2019, 141, 16624-16634.	13.7	47
70	Lead–Oxygen Bond Length Distributions of the Relaxor Ferroelectric 0.67PbMg1/3Nb2/3O3–0.33PbTiO3 from 207Pb Nuclear Magnetic Resonance. Journal of Physical Chemistry C, 2019, 123, 15744-15750.	3.1	5
71	Multifunctional Molecular Modulation for Efficient and Stable Hybrid Perovskite Solar Cells. Chimia, 2019, 73, 317.	0.6	19
72	Nucleobase pairing and photodimerization in a biologically derived metal-organic framework nanoreactor. Nature Communications, 2019, 10, 1612.	12.8	58

#	Article	IF	CITATIONS
73	Supramolecular Engineering for Formamidiniumâ€Based Layered 2D Perovskite Solar Cells: Structural Complexity and Dynamics Revealed by Solidâ€&tate NMR Spectroscopy. Advanced Energy Materials, 2019, 9, 1900284.	19.5	89
74	<sup>19</sup> F Magic Angle Spinning Dynamic Nuclear Polarization Enhanced NMR Spectroscopy. Angewandte Chemie - International Edition, 2019, 58, 7249-7253.	13.8	18
75	One- and Two-Dimensional High-Resolution NMR from Flat Surfaces. ACS Central Science, 2019, 5, 515-523.	11.3	17
76	Topology of Pretreated Wood Fibers Using Dynamic Nuclear Polarization. Journal of Physical Chemistry C, 2019, 123, 30407-30415.	3.1	22
77	A Bayesian approach to NMR crystal structure determination. Physical Chemistry Chemical Physics, 2019, 21, 23385-23400.	2.8	39
78	Doping and phase segregation in Mn <sup>2+</sup> - and Co <sup>2+</sup> -doped lead halide perovskites from <sup>133</sup> Cs and <sup>1</sup> H NMR relaxation enhancement. Journal of Materials Chemistry A, 2019, 7, 2326-2333.	10.3	59
79	Europium-Doped CsPbI2Br for Stable and Highly Efficient Inorganic Perovskite Solar Cells. Joule, 2019, 3, 205-214.	24.0	387
80	Elucidating an Amorphous Form Stabilization Mechanism for Tenapanor Hydrochloride: Crystal Structure Analysis Using X-ray Diffraction, NMR Crystallography, and Molecular Modeling. Molecular Pharmaceutics, 2018, 15, 1476-1487.	4.6	32
81	DNP enhanced NMR with flip-back recovery. Journal of Magnetic Resonance, 2018, 288, 69-75.	2.1	19
82	Formation of Stable Mixed Guanidinium–Methylammonium Phases with Exceptionally Long Carrier Lifetimes for High-Efficiency Lead Iodide-Based Perovskite Photovoltaics. Journal of the American Chemical Society, 2018, 140, 3345-3351.	13.7	235
83	Structure of Lipid Nanoparticles Containing siRNA or mRNA by Dynamic Nuclear Polarization-Enhanced NMR Spectroscopy. Journal of Physical Chemistry B, 2018, 122, 2073-2081.	2.6	121
84	One-step mechanochemical incorporation of an insoluble cesium additive for high performance planar heterojunction solar cells. Nano Energy, 2018, 49, 523-528.	16.0	95
85	Conformational dynamics in crystals reveal the molecular bases for D76N beta-2 microglobulin aggregation propensity. Nature Communications, 2018, 9, 1658.	12.8	53
86	Predicting the DNP-SENS efficiency in reactive heterogeneous catalysts from hydrophilicity. Chemical Science, 2018, 9, 4866-4872.	7.4	24
87	Hyperpolarized long-lived nuclear spin states in monodeuterated methyl groups. Physical Chemistry Chemical Physics, 2018, 20, 9755-9759.	2.8	23
88	DNPâ€enhanced solidâ€state NMR spectroscopy of active pharmaceutical ingredients. Magnetic Resonance in Chemistry, 2018, 56, 583-609.	1.9	61
89	Addition of adamantylammonium iodide to hole transport layers enables highly efficient and electroluminescent perovskite solar cells. Energy and Environmental Science, 2018, 11, 3310-3320.	30.8	137
90	Probing Protein Dynamics Using Multifield Variable Temperature NMR Relaxation and Molecular Dynamics Simulation. Journal of Physical Chemistry B, 2018, 122, 9697-9702.	2.6	15

#	Article	IF	CITATIONS
91	BDPA-Nitroxide Biradicals Tailored for Efficient Dynamic Nuclear Polarization Enhanced Solid-State NMR at Magnetic Fields up to 21.1 T. Journal of the American Chemical Society, 2018, 140, 13340-13349.	13.7	99
92	Multifunctional molecular modulators for perovskite solar cells with over 20% efficiency and high operational stability. Nature Communications, 2018, 9, 4482.	12.8	266
93	Core–Shell Structure of Organic Crystalline Nanoparticles Determined by Relayed Dynamic Nuclear Polarization NMR. Journal of Physical Chemistry A, 2018, 122, 8802-8807.	2.5	22
94	Chemical shifts in molecular solids by machine learning. Nature Communications, 2018, 9, 4501.	12.8	170
95	Phase Segregation in Potassium-Doped Lead Halide Perovskites from <sup>39</sup> K Solid-State NMR at 21.1 T. Journal of the American Chemical Society, 2018, 140, 7232-7238.	13.7	130
96	Bulk Nuclear Hyperpolarization of Inorganic Solids by Relay from the Surface. Journal of the American Chemical Society, 2018, 140, 7946-7951.	13.7	50
97	Refocused linewidths less than 10†Hz in 1H solid-state NMR. Journal of Magnetic Resonance, 2018, 293, 41-46.	2.1	5
98	Resolving the Core and the Surface of CdSe Quantum Dots and Nanoplatelets Using Dynamic Nuclear Polarization Enhanced PASS–PIETA NMR Spectroscopy. ACS Central Science, 2018, 4, 1113-1125.	11.3	46
99	Transportable hyperpolarized metabolites. Nature Communications, 2017, 8, 13975.	12.8	86
100	Positional Variance in NMR Crystallography. Journal of the American Chemical Society, 2017, 139, 2573-2576.	13.7	48
101	Oxygen-17 dynamic nuclear polarisation enhanced solid-state NMR spectroscopy at 18.8 T. Chemical Communications, 2017, 53, 2563-2566.	4.1	39
102	Donor–acceptor stacking arrangements in bulk and thin-film high-mobility conjugated polymers characterized using molecular modelling and MAS and surface-enhanced solid-state NMR spectroscopy. Chemical Science, 2017, 8, 3126-3136.	7.4	64
103	Solvent suppression in DNP enhanced solid state NMR. Journal of Magnetic Resonance, 2017, 277, 149-153.	2.1	31
104	Improving Sensitivity of Solid-state NMR Spectroscopy by Rational Design of Polarizing Agents for Dynamic Nuclear Polarization. Chimia, 2017, 71, 190-194.	0.6	4
105	Tailored Polarizing Hybrid Solids with Nitroxide Radicals Localized in Mesostructured Silica Walls. Helvetica Chimica Acta, 2017, 100, e1700101.	1.6	24
106	Does Z′ equal 1 or 2? Enhanced powder NMR crystallography verification of a disordered room temperature crystal structure of a p38 inhibitor for chronic obstructive pulmonary disease. Physical Chemistry Chemical Physics, 2017, 19, 16650-16661.	2.8	25
107	Frozen Acrylamide Gels as Dynamic Nuclear Polarization Matrices. Angewandte Chemie - International Edition, 2017, 56, 8726-8730.	13.8	26
108	Cation Dynamics in Mixed-Cation (MA) <sub><i>x</i></sub> (FA) <sub>1–<i>x</i></sub> Pbl <sub>3</sub> Hybrid Perovskites from Solid-State NMR. Journal of the American Chemical Society, 2017, 139, 10055-10061.	13.7	209

#	Article	IF	CITATIONS
109	Paramagnetic Properties of a Crystalline Iron–Sulfur Protein by Magic-Angle Spinning NMR Spectroscopy. Inorganic Chemistry, 2017, 56, 6624-6629.	4.0	19
110	The Atomic-Level Structure of Cementitious Calcium Silicate Hydrate. Journal of Physical Chemistry C, 2017, 121, 17188-17196.	3.1	178
111	The structure and binding mode of citrate in the stabilization of gold nanoparticles. Nature Chemistry, 2017, 9, 890-895.	13.6	222
112	Three-Dimensional Structure Determination of Surface Sites. Journal of the American Chemical Society, 2017, 139, 849-855.	13.7	75
113	Determining the Surface Structure of Silicated Alumina Catalysts via Isotopic Enrichment and Dynamic Nuclear Polarization Surface-Enhanced NMR Spectroscopy. Journal of Physical Chemistry C, 2017, 121, 22977-22984.	3.1	34
114	Phase Segregation in Cs-, Rb- and K-Doped Mixed-Cation (MA) <sub><i>x</i></sub> (FA) <sub>1–<i>x</i></sub> PbI <sub>3</sub> Hybrid Perovskites from Solid-State NMR. Journal of the American Chemical Society, 2017, 139, 14173-14180.	13.7	317
115	Frozen Acrylamide Gels as Dynamic Nuclear Polarization Matrices. Angewandte Chemie, 2017, 129, 8852-8856.	2.0	2
116	Structure of outer membrane protein G in lipid bilayers. Nature Communications, 2017, 8, 2073.	12.8	91
117	Dynamic Nuclear Polarization Efficiency Increased by Very Fast Magic Angle Spinning. Journal of the American Chemical Society, 2017, 139, 10609-10612.	13.7	52
118	Measuring Nano- to Microstructures from Relayed Dynamic Nuclear Polarization NMR. Journal of Physical Chemistry C, 2017, 121, 15993-16005.	3.1	88
119	Local Structures and Heterogeneity of Silica-Supported M(III) Sites Evidenced by EPR, IR, NMR, and Luminescence Spectroscopies. Journal of the American Chemical Society, 2017, 139, 8855-8867.	13.7	58
120	Reactive surface organometallic complexes observed using dynamic nuclear polarization surface enhanced NMR spectroscopy. Chemical Science, 2017, 8, 284-290.	7.4	55
121	Dendritic polarizing agents for DNP SENS. Chemical Science, 2017, 8, 416-422.	7.4	35
122	Atomistic Description of Reaction Intermediates for Supported Metathesis Catalysts Enabled by DNP SENS. Angewandte Chemie, 2016, 128, 4821-4825.	2.0	6
123	Monolayer Doping of Silicon through Grafting a Tailored Molecular Phosphorus Precursor onto Oxide-Passivated Silicon Surfaces. Chemistry of Materials, 2016, 28, 3634-3640.	6.7	50
124	Structure elucidation of a complex CO <sub>2</sub> -based organic framework material by NMR crystallography. Chemical Science, 2016, 7, 4379-4390.	7.4	39
125	Correlating Synthetic Methods, Morphology, Atomic-Level Structure, and Catalytic Activity of Sn-β Catalysts. ACS Catalysis, 2016, 6, 4047-4063.	11.2	106
126	Molecular Level Characterization of the Structure and Interactions in Peptideâ€Functionalized Metal–Organic Frameworks. Chemistry - A European Journal, 2016, 22, 16531-16538.	3.3	27

#	Article	IF	CITATIONS
127	<sup>35</sup> Cl dynamic nuclear polarization solid-state NMR of active pharmaceutical ingredients. Physical Chemistry Chemical Physics, 2016, 18, 25893-25904.	2.8	87
128	Structure of fully protonated proteins by proton-detected magic-angle spinning NMR. Proceedings of the United States of America, 2016, 113, 9187-9192.	7.1	224
129	Hyperpolarization of Frozen Hydrocarbon Gases by Dynamic Nuclear Polarization at 1.2 K. Journal of Physical Chemistry Letters, 2016, 7, 3235-3239.	4.6	18
130	Atomistic Description of Reaction Intermediates for Supported Metathesis Catalysts Enabled by DNP SENS. Angewandte Chemie - International Edition, 2016, 55, 4743-4747.	13.8	52
131	Weak and Transient Protein Interactions Determined by Solidâ€State NMR. Angewandte Chemie - International Edition, 2016, 55, 6638-6641.	13.8	28
132	Atomic-level organization of vicinal acid–base pairs through the chemisorption of aniline and derivatives onto mesoporous SBA15. Chemical Science, 2016, 7, 6099-6105.	7.4	16
133	Weak and Transient Protein Interactions Determined by Solidâ€State NMR. Angewandte Chemie, 2016, 128, 6750-6753.	2.0	14
134	Dynamic nuclear polarization at 40 kHz magic angle spinning. Physical Chemistry Chemical Physics, 2016, 18, 10616-10622.	2.8	74
135	Rational design of dinitroxide biradicals for efficient cross-effect dynamic nuclear polarization. Chemical Science, 2016, 7, 550-558.	7.4	141
136	Iridium(I)/Nâ€Heterocyclic Carbene Hybrid Materials: Surface Stabilization of Lowâ€Valent Iridium Species for High Catalytic Hydrogenation Performance. Angewandte Chemie - International Edition, 2015, 54, 12937-12941.	13.8	33
137	Solid-State Dynamic Nuclear Polarization at 9.4 and 18.8 T from 100 K to Room Temperature. Journal of the American Chemical Society, 2015, 137, 14558-14561.	13.7	87
138	Lipid bilayer-bound conformation of an integral membrane beta barrel protein by multidimensional MAS NMR. Journal of Biomolecular NMR, 2015, 61, 299-310.	2.8	38
139	Alkane Metathesis with the Tantalum Methylidene [(≡SiO)Ta(â•CH <sub>2</sub> )Me <sub>2</sub> ]/[(≡SiO) <sub>2</sub> Ta(â•CH <sub>2</sub> )Me] Gener from Well-Defined Surface Organometallic Complex [(≡SiO)Ta <sup>V</sup> Me <sub>4</sub> ]. Journal of the American Chemical Society. 2015. 137. 588-591.	ated 13.7	65
140	Atomistic Description of Thiostannate-Capped CdSe Nanocrystals: Retention of Four-Coordinate SnS4 Motif and Preservation of Cd-Rich Stoichiometry. Journal of the American Chemical Society, 2015, 137, 1862-1874.	13.7	48
141	Sensitivity and resolution of proton detected spectra of a deuterated protein at 40 and 60ÂkHz magic-angle-spinning. Journal of Biomolecular NMR, 2015, 61, 161-171.	2.8	34
142	Protein residue linking in a single spectrum for magic-angle spinning NMR assignment. Journal of Biomolecular NMR, 2015, 62, 253-261.	2.8	44
143	Influences of Dilute Organic Adsorbates on the Hydration of Low-Surface-Area Silicates. Journal of the American Chemical Society, 2015, 137, 8096-8112.	13.7	85
144	Structure and Mechanism of the Influenza A M2 <sub>18–60</sub> Dimer of Dimers. Journal of the American Chemical Society, 2015, 137, 14877-14886.	13.7	103

#	Article	IF	CITATIONS
145	Direct observation of hierarchical protein dynamics. Science, 2015, 348, 578-581.	12.6	222
146	Macroscopic nuclear spin diffusion constants of rotating polycrystalline solids from first-principles simulation. Journal of Magnetic Resonance, 2015, 254, 48-55.	2.1	18
147	Cooperative Effect of Monopodal Silica-Supported Niobium Complex Pairs Enhancing Catalytic Cyclic Carbonate Production. Journal of the American Chemical Society, 2015, 137, 7728-7739.	13.7	123
148	Superstructure of a Substituted Zeolitic Imidazolate Metal–Organic Framework Determined by Combining Proton Solid‧tate NMR Spectroscopy and DFT Calculations. Angewandte Chemie - International Edition, 2015, 54, 5971-5976.	13.8	38
149	High-resolution NMR of hydrogen in organic solids by DNP enhanced natural abundance deuterium spectroscopy. Journal of Magnetic Resonance, 2015, 259, 192-198.	2.1	26
150	Nanostructure of Materials Determined by Relayed Paramagnetic Relaxation Enhancement. Journal of the American Chemical Society, 2015, 137, 12482-12485.	13.7	19
151	Polymorphs of Theophylline Characterized by DNP Enhanced Solid-State NMR. Molecular Pharmaceutics, 2015, 12, 4146-4153.	4.6	77
152	Structure of Colloidal Quantum Dots from Dynamic Nuclear Polarization Surface Enhanced NMR Spectroscopy. Journal of the American Chemical Society, 2015, 137, 13964-13971.	13.7	105
153	Atomic Description of the Interface between Silica and Alumina in Aluminosilicates through Dynamic Nuclear Polarization Surface-Enhanced NMR Spectroscopy and First-Principles Calculations. Journal of the American Chemical Society, 2015, 137, 10710-10719.	13.7	129
154	A solid-state NMR method to determine domain sizes in multi-component polymer formulations. Journal of Magnetic Resonance, 2015, 261, 43-48.	2.1	14
155	Highâ€Resolution <sup>1</sup> H Solidâ€6tate NMR Spectroscopy Using Windowed LG4 Homonuclear Dipolar Decoupling. Israel Journal of Chemistry, 2014, 54, 136-146.	2.3	13
156	NMR Signatures of the Active Sites in Snâ€Î²â€Zeolite. Angewandte Chemie, 2014, 126, 10343-10347.	2.0	46
157	Silica-surface reorganization during organotin grafting evidenced by 119Sn DNP SENS: a tandem reaction of gem-silanols and strained siloxane bridges. Physical Chemistry Chemical Physics, 2014, 16, 17822-17827.	2.8	40
158	Metabolic expressivity of human genetic variants: NMR metabotyping of MEN1 pathogenic mutants. Journal of Pharmaceutical and Biomedical Analysis, 2014, 93, 118-124.	2.8	4
159	Dynamic Nuclear Polarization Enhanced NMR Spectroscopy for Pharmaceutical Formulations. Journal of the American Chemical Society, 2014, 136, 2324-2334.	13.7	145
160	Amplifying Dynamic Nuclear Polarization of Frozen Solutions by Incorporating Dielectric Particles. Journal of the American Chemical Society, 2014, 136, 15711-15718.	13.7	103
161	NMR Signatures of the Active Sites in Snâ€Î²â€Zeolite. Angewandte Chemie - International Edition, 2014, 53, 10179-10183.	13.8	157
162	Homonuclear Decoupling of <sup>1</sup> H Dipolar Interactions in Solids by means of Heteronuclear Recoupling. Israel Journal of Chemistry, 2014, 54, 154-162.	2.3	2

#	Article	IF	CITATIONS
163	Sn surface-enriched Pt–Sn bimetallic nanoparticles as a selective and stable catalyst for propane dehydrogenation. Journal of Catalysis, 2014, 320, 52-62.	6.2	144
164	Dynamic nuclear polarisation enhanced14N overtone MAS NMR spectroscopy. Physical Chemistry Chemical Physics, 2014, 16, 12890-12899.	2.8	35
165	Hydrophobic radicals embedded in neutral surfactants for dynamic nuclear polarization of aqueous environments at 9.4 Tesla. Chemical Communications, 2014, 50, 10198-10201.	4.1	23
166	Hybrid polarizing solids for pure hyperpolarized liquids through dissolution dynamic nuclear polarization. Proceedings of the National Academy of Sciences of the United States of America, 2014, 111, 14693-14697.	7.1	93
167	WMe6 Tamed by Silica: ≡Si–O–WMe5 as an Efficient, Well-Defined Species for Alkane Metathesis, Leading to the Observation of a Supported W–Methyl/Methylidyne Species. Journal of the American Chemical Society, 2014, 136, 1054-1061.	13.7	84
168	Unraveling the Core–Shell Structure of Ligand-Capped Sn/SnOxNanoparticles by Surface-Enhanced Nuclear Magnetic Resonance, Mössbauer, and X-ray Absorption Spectroscopies. ACS Nano, 2014, 8, 2639-2648.	14.6	87
169	Characterising local environments in high energy density Li-ion battery cathodes: a combined NMR and first principles study of LiFe <sub>x</sub> Co <sub>1â^*x</sub> PO <sub>4</sub> . Journal of Materials Chemistry A, 2014, 2, 11948-11957.	10.3	50
170	Insights into the Structure and Dynamics of Measles Virus Nucleocapsids by 1H-detected Solid-state NMR. Biophysical Journal, 2014, 107, 941-946.	0.5	30
171	Rapid Proton-Detected NMR Assignment for Proteins with Fast Magic Angle Spinning. Journal of the American Chemical Society, 2014, 136, 12489-12497.	13.7	254
172	Heteronuclear proton double quantum-carbon single quantum scalar correlation in solids. Journal of Magnetic Resonance, 2014, 245, 31-37.	2.1	10
173	Well-defined mono(η3-allyl)nickel complex î€,MONi(η3-C3H5) (M = Si or Al) grafted onto silica or alumina: a molecularly dispersed nickel precursor for syntheses of supported small size nickel nanoparticles. Chemical Communications, 2014, 50, 7716.	4.1	12
174	A Wellâ€Defined Pd Hybrid Material for the <i>Z</i> â€Selective Semihydrogenation of Alkynes Characterized at the Molecular Level by DNP SENS. Chemistry - A European Journal, 2013, 19, 12234-12238.	3.3	61
175	Bipodal Surface Organometallic Complexes with Surface N-Donor Ligands and Application to the Catalytic Cleavage of C–H and C–C Bonds in n-Butane. Journal of the American Chemical Society, 2013, 135, 17943-17951.	13.7	33
176	<i>De Novo</i> Determination of the Crystal Structure of a Large Drug Molecule by Crystal Structure Prediction-Based Powder NMR Crystallography. Journal of the American Chemical Society, 2013, 135, 17501-17507.	13.7	173
177	A Well-Defined Silica-Supported Tungsten Oxo Alkylidene Is a Highly Active Alkene Metathesis Catalyst. Journal of the American Chemical Society, 2013, 135, 19068-19070.	13.7	83
178	Frontiers in Solid-State NMR Technology. Accounts of Chemical Research, 2013, 46, 1912-1913.	15.6	19
179	Solid-Phase Polarization Matrixes for Dynamic Nuclear Polarization from Homogeneously Distributed Radicals in Mesostructured Hybrid Silica Materials. Journal of the American Chemical Society, 2013, 135, 15459-15466.	13.7	56
180	Methane Reacts with Heteropolyacids Chemisorbed on Silica to Produce Acetic Acid under Soft Conditions. Journal of the American Chemical Society, 2013, 135, 804-810.	13.7	24

#	Article	IF	CITATIONS
181	Improved Dynamic Nuclear Polarization Surfaceâ€Enhanced NMR Spectroscopy through Controlled Incorporation of Deuterated Functional Groups. Angewandte Chemie - International Edition, 2013, 52, 1222-1225.	13.8	58
182	Powder crystallography of pharmaceutical materials by combined crystal structure prediction and solid-state 1H NMR spectroscopy. Physical Chemistry Chemical Physics, 2013, 15, 8069.	2.8	155
183	Magic Angle Spinning NMR of Paramagnetic Proteins. Accounts of Chemical Research, 2013, 46, 2108-2116.	15.6	78
184	Molecular-level characterization of the structure and the surface chemistry of periodic mesoporous organosilicates using DNP-surface enhanced NMR spectroscopy. Physical Chemistry Chemical Physics, 2013, 15, 13270.	2.8	56
185	Frequency-stepped acquisition in nuclear magnetic resonance spectroscopy under magic angle spinning. Journal of Chemical Physics, 2013, 138, 114201.	3.0	40
186	<sup>13</sup> Câ€Detected Throughâ€Bond Correlation Experiments for Protein Resonance Assignment by Ultraâ€Fast MAS Solidâ€State NMR. ChemPhysChem, 2013, 14, 3131-3137.	2.1	19
187	Dynamic Nuclear Polarization Surface Enhanced NMR Spectroscopy. Accounts of Chemical Research, 2013, 46, 1942-1951.	15.6	524
188	Evidence for Metal–Surface Interactions and Their Role in Stabilizing Well-Defined Immobilized Ru–NHC Alkene Metathesis Catalysts. Journal of the American Chemical Society, 2013, 135, 3193-3199.	13.7	96
189	Out-and-back 13C–13C scalar transfers in protein resonance assignment by proton-detected solid-state NMR under ultra-fast MAS. Journal of Biomolecular NMR, 2013, 56, 379-386.	2.8	54
190	Advances in Magnetic Resonance: From Stem Cells to Catalytic Surfaces. Journal of the American Chemical Society, 2013, 135, 8089-8091.	13.7	9
191	Large Molecular Weight Nitroxide Biradicals Providing Efficient Dynamic Nuclear Polarization at Temperatures up to 200 K. Journal of the American Chemical Society, 2013, 135, 12790-12797.	13.7	355
192	Improved Phase-Modulated Homonuclear Dipolar Decoupling for Solid-State NMR Spectroscopy from Symmetry Considerations. Journal of Physical Chemistry A, 2013, 117, 5280-5290.	2.5	20
193	Structure and backbone dynamics of a microcrystalline metalloprotein by solid-state NMR. Proceedings of the National Academy of Sciences of the United States of America, 2012, 109, 11095-11100.	7.1	173
194	Quasi-equilibria in reduced Liouville spaces. Journal of Chemical Physics, 2012, 136, 224511.	3.0	14
195	Backbone Assignment of Fully Protonated Solid Proteins by <sup>1</sup> H Detection and Ultrafast Magicâ€Angleâ€Spinning NMR Spectroscopy. Angewandte Chemie - International Edition, 2012, 51, 10756-10759.	13.8	95
196	Rapid Measurement of Pseudocontact Shifts in Metalloproteins by Proton-Detected Solid-State NMR Spectroscopy. Journal of the American Chemical Society, 2012, 134, 14730-14733.	13.7	53
197	A first-principles description of proton-driven spin diffusion. Physical Chemistry Chemical Physics, 2012, 14, 86-89.	2.8	20
198	Atomic-Resolution Structural Dynamics in Crystalline Proteins from NMR and Molecular Simulation. Journal of Physical Chemistry Letters, 2012, 3, 3657-3662.	4.6	47

#	Article	IF	CITATIONS
199	A Slowly Relaxing Rigid Biradical for Efficient Dynamic Nuclear Polarization Surface-Enhanced NMR Spectroscopy: Expeditious Characterization of Functional Group Manipulation in Hybrid Materials. Journal of the American Chemical Society, 2012, 134, 2284-2291.	13.7	182
200	Dynamic Nuclear Polarization NMR Spectroscopy of Microcrystalline Solids. Journal of the American Chemical Society, 2012, 134, 16899-16908.	13.7	242
201	Spin-Transfer Pathways in Paramagnetic Lithium Transition-Metal Phosphates from Combined Broadband Isotropic Solid-State MAS NMR Spectroscopy and DFT Calculations. Journal of the American Chemical Society, 2012, 134, 17178-17185.	13.7	122
202	A Silica-Supported Double-Decker Silsesquioxane Provides a Second Skin for the Selective Generation of Bipodal Surface Organometallic Complexes. Organometallics, 2012, 31, 7610-7617.	2.3	22
203	A well-defined mesoporous amine silica surface via a selective treatment of SBA-15 with ammonia. Chemical Communications, 2012, 48, 3067.	4.1	25
204	Dynamic nuclear polarization of quadrupolar nuclei using cross polarization from protons: surface-enhanced aluminium-27 NMR. Chemical Communications, 2012, 48, 1988.	4.1	123
205	Non-aqueous solvents for DNP surface enhanced NMR spectroscopy. Chemical Communications, 2012, 48, 654-656.	4.1	155
206	One hundred fold overall sensitivity enhancements for Silicon-29 NMR spectroscopy of surfaces by dynamic nuclear polarization with CPMG acquisition. Chemical Science, 2012, 3, 108-115.	7.4	141
207	Combination of DQ and ZQ Coherences for Sensitive Throughâ€Bond NMR Correlation Experiments in Biosolids under Ultraâ€Fast MAS. ChemPhysChem, 2012, 13, 2405-2411.	2.1	21
208	A common theory for phase-modulated homonuclear decoupling in solid-state NMR. Physical Chemistry Chemical Physics, 2012, 14, 9121.	2.8	13
209	Dynamic Nuclear Polarization Enhanced Solid‣tate NMR Spectroscopy of Functionalized Metal–Organic Frameworks. Angewandte Chemie - International Edition, 2012, 51, 123-127.	13.8	161
210	High-resolution and sensitivity through-bond correlations in ultra-fast magic angle spinning (MAS) solid-state NMR. Chemical Science, 2011, 2, 345-348.	7.4	38
211	Single crystal nuclear magnetic resonance in spinning powders. Journal of Chemical Physics, 2011, 135, 144201.	3.0	14
212	A master-equation approach to the description of proton-driven spin diffusion from crystal geometry using simulated zero-quantum lineshapes. Physical Chemistry Chemical Physics, 2011, 13, 7363.	2.8	24
213	Probing surface site heterogeneity through 1D and INADEQUATE 31P solid state NMR spectroscopy of silica supported PMe3-Au(I) adducts. Chemical Science, 2011, 2, 928.	7.4	15
214	Broad-Ranging Natural Metabotype Variation Drives Physiological Plasticity in Healthy Control Inbred Rat Strains. Journal of Proteome Research, 2011, 10, 1675-1689.	3.7	19
215	Fast Characterization of Functionalized Silica Materials by Silicon-29 Surface-Enhanced NMR Spectroscopy Using Dynamic Nuclear Polarization. Journal of the American Chemical Society, 2011, 133, 2104-2107.	13.7	254
216	A highly ordered mesostructured material containing regularly distributed phenols: preparation and characterization at a molecular level through ultra-fast magic angle spinning proton NMR spectroscopy. Physical Chemistry Chemical Physics, 2011, 13, 4230.	2.8	13

#	Article	IF	CITATIONS
217	Enhanced Resolution and Coherence Lifetimes in the Solid-State NMR Spectroscopy of Perdeuterated Proteins under Ultrafast Magic-Angle Spinning. Journal of Physical Chemistry Letters, 2011, 2, 2205-2211.	4.6	123
218	A scaling factor theorem for homonuclear dipolar decoupling in solid-state NMR spectroscopy. Journal of Magnetic Resonance, 2011, 212, 11-16.	2.1	8
219	Site-Specific Measurement of Slow Motions in Proteins. Journal of the American Chemical Society, 2011, 133, 16762-16765.	13.7	105
220	Orthogonal Filtered Recoupled-STOCSY to Extract Metabolic Networks Associated with Minor Perturbations from NMR Spectroscopy. Journal of Proteome Research, 2011, 10, 4342-4348.	3.7	27
221	Fast Resonance Assignment and Fold Determination of Human Superoxide Dismutase by Highâ€Resolution Protonâ€Detected Solidâ€6tate MAS NMR Spectroscopy. Angewandte Chemie - International Edition, 2011, 50, 11697-11701.	13.8	157
222	Broadband inversion for MAS NMR with single-sideband-selective adiabatic pulses. Journal of Chemical Physics, 2011, 134, 024117.	3.0	41
223	Powder Crystallography by Combined Crystal Structure Prediction and High-Resolution <sup>1</sup> H Solid-State NMR Spectroscopy. Journal of the American Chemical Society, 2010, 132, 2564-2566.	13.7	201
224	Two-Dimensional Statistical Recoupling for the Identification of Perturbed Metabolic Networks from NMR Spectroscopy. Journal of Proteome Research, 2010, 9, 4513-4520.	3.7	47
225	Computation and NMR crystallography of terbutaline sulfate. Magnetic Resonance in Chemistry, 2010, 48, S103-S112.	1.9	76
226	Targeted projection NMR spectroscopy for unambiguous metabolic profiling of complex mixtures. Magnetic Resonance in Chemistry, 2010, 48, 727-733.	1.9	17
227	Homonuclear dipolar decoupling with very large scaling factors for high-resolution ultrafast magic angle spinning 1H solid-state NMR spectroscopy. Chemical Physics Letters, 2010, 498, 214-220.	2.6	39
228	Surface Enhanced NMR Spectroscopy by Dynamic Nuclear Polarization. Journal of the American Chemical Society, 2010, 132, 15459-15461.	13.7	488
229	Ab initio simulation of proton spin diffusion. Physical Chemistry Chemical Physics, 2010, 12, 9172.	2.8	34
230	Fibrillar vs Crystalline Full-Length β-2-Microglobulin Studied by High-Resolution Solid-State NMR Spectroscopy. Journal of the American Chemical Society, 2010, 132, 5556-5557.	13.7	32
231	Ultrafast MAS Solid-State NMR Permits Extensive <sup>13</sup> C and <sup>1</sup> H Detection in Paramagnetic Metalloproteins. Journal of the American Chemical Society, 2010, 132, 5558-5559.	13.7	109
232	Complete 1H resonance assignment of β-maltose from 1H–1H DQ-SQ CRAMPS and 1H (DQ-DUMBO)–13C refocused INEPT 2D solid-state NMR spectra and first principles GIPAW calculations. Physical Chemistry Chemical Physics, 2010, 12, 6970.	SQ 2.8	83
233	Anisotropic Collective Motion Contributes to Nuclear Spin Relaxation in Crystalline Proteins. Journal of the American Chemical Society, 2010, 132, 1246-1248.	13.7	43
234	Numerical simulation of free evolution in solid-state nuclear magnetic resonance using low-order correlations in Liouville space. Journal of Chemical Physics, 2010, 133, 224501.	3.0	29

LYNDON EMSLEY

#	Article	IF	CITATIONS
235	Synthesis and reactivity of molybdenum imido alkylidene bis-pyrazolide complexes. Dalton Transactions, 2010, 39, 8547.	3.3	18
236	NMR Crystallography of Campho[2,3-c]pyrazole ( <i>Z</i> ′ = 6): Combining High-Resolution <sup>1</sup> H- <sup>13</sup> C Solid-State MAS NMR Spectroscopy and GIPAW Chemical-Shift Calculations. Journal of Physical Chemistry A, 2010, 114, 10435-10442.	2.5	127
237	Measurement of Site-Specific <sup>13</sup> C Spinâ^'Lattice Relaxation in a Crystalline Protein. Journal of the American Chemical Society, 2010, 132, 8252-8254.	13.7	80
238	Wellâ€Defined Silicaâ€Supported Mo–Alkylidene Catalyst Precursors Containing One OR Substituent: Methods of Preparation and Structure–Reactivity Relationship in Alkene Metathesis. Chemistry - A European Journal, 2009, 15, 5083-5089.	3.3	53
239	Crystalâ€6tructure Determination of Powdered Paramagnetic Lanthanide Complexes by Proton NMR Spectroscopy. Angewandte Chemie - International Edition, 2009, 48, 3082-3086.	13.8	63
240	Characterization of different water pools in solid-state NMR protein samples. Journal of Biomolecular NMR, 2009, 45, 319-327.	2.8	239
241	Fast acquisition of multi-dimensional spectra in solid-state NMR enabled by ultra-fast MAS. Journal of Magnetic Resonance, 2009, 196, 133-141.	2.1	109
242	Enhanced sensitivity in high-resolution 1H solid-state NMR spectroscopy with DUMBO dipolar decoupling under ultra-fast MAS. Chemical Physics Letters, 2009, 469, 336-341.	2.6	80
243	Dynamics of large nuclear-spin systems from low-order correlations in Liouville space. Chemical Physics Letters, 2009, 477, 377-381.	2.6	39
244	Motional heterogeneity in single-site silica-supported species revealed by deuteron NMR. Physical Chemistry Chemical Physics, 2009, 11, 6962.	2.8	27
245	Statistical Recoupling Prior to Significance Testing in Nuclear Magnetic Resonance Based Metabonomics. Analytical Chemistry, 2009, 81, 6242-6251.	6.5	88
246	Transverse-Dephasing Optimized Homonuclear J-Decoupling in Solid-State NMR Spectroscopy of Uniformly 13C-Labeled Proteins. Journal of the American Chemical Society, 2009, 131, 10816-10817.	13.7	36
247	Metabolic Profiling Strategy of <i>Caenorhabditis elegans</i> by Whole-Organism Nuclear Magnetic Resonance. Journal of Proteome Research, 2009, 8, 2542-2550.	3.7	51
248	Powder NMR crystallography of thymol. Physical Chemistry Chemical Physics, 2009, 11, 2610.	2.8	180
249	Characterizing Slight Structural Disorder in Solids by Combined Solid-State NMR and First Principles Calculations. Journal of Physical Chemistry A, 2009, 113, 902-911.	2.5	47
250	Gold Nanoparticles Supported on Passivated Silica: Access to an Efficient Aerobic Epoxidation Catalyst and the Intrinsic Oxidation Activity of Gold. Journal of the American Chemical Society, 2009, 131, 14667-14669.	13.7	111
251	Polarization Transfer over the Water–Protein Interface in Solids. Angewandte Chemie - International Edition, 2008, 47, 5851-5854.	13.8	44
252	Resonator with reduced sample heating and increased homogeneity for solid-state NMR. Journal of Magnetic Resonance, 2008, 191, 78-92.	2.1	30

LYNDON EMSLEY

#	Article	IF	CITATIONS
253	Improving resolution in proton solid-state NMR by removing nitrogen-14 residual dipolar broadening. Chemical Physics Letters, 2008, 458, 391-395.	2.6	9
254	Methyl Proton Contacts Obtained Using Heteronuclear Through-Bond Transfers in Solid-State NMR Spectroscopy. Journal of the American Chemical Society, 2008, 130, 10625-10632.	13.7	19
255	Superadiabaticity in magnetic resonance. Journal of Chemical Physics, 2008, 129, 204110.	3.0	49
256	Band-Selective <sup>1</sup> Hâ^' <sup>13</sup> C Cross-Polarization in Fast Magic Angle Spinning Solid-State NMR Spectroscopy. Journal of the American Chemical Society, 2008, 130, 17216-17217.	13.7	81
257	High resolution solid state NMRspectroscopy in surface organometallic chemistry: access to molecular understanding of active sites of well-defined heterogeneous catalysts. Chemical Society Reviews, 2008, 37, 518-526.	38.1	97
258	Dynamics and Disorder in Surfactant-Templated Silicate Layers Studied by Solid-State NMR Dephasing Times and Correlated Line Shapes. Journal of Physical Chemistry C, 2008, 112, 9145-9154.	3.1	46
259	Dynamics of Silica-Supported Catalysts Determined by Combining Solid-State NMR Spectroscopy and DFT Calculations. Journal of the American Chemical Society, 2008, 130, 5886-5900.	13.7	98
260	Direct observation of reaction intermediates for a well defined heterogeneous alkene metathesis catalyst. Proceedings of the National Academy of Sciences of the United States of America, 2008, 105, 12123-12127.	7.1	86
261	Metabotyping of <i>Caenorhabditis elegans</i> reveals latent phenotypes. Proceedings of the National Academy of Sciences of the United States of America, 2007, 104, 19808-19812.	7.1	107
262	Resolving Structures from Powders by NMR Crystallography Using Combined Proton Spin Diffusion and Plane Wave DFT Calculations. Journal of the American Chemical Society, 2007, 129, 8932-8933.	13.7	120
263	NMRcrystallography of oxybuprocaine hydrochloride, Modification II°. Physical Chemistry Chemical Physics, 2007, 9, 360-368.	2.8	102
264	NMR measurements of scalar-coupling distributions in disordered solids. Physical Chemistry Chemical Physics, 2007, 9, 92-103.	2.8	33
265	Well-Defined Surface Imido Amido Tantalum(V) Species from Ammonia and Silica-Supported Tantalum Hydrides. Journal of the American Chemical Society, 2007, 129, 176-186.	13.7	79
266	Absence of Curie Relaxation in Paramagnetic Solids Yields Long1H Coherence Lifetimes. Journal of the American Chemical Society, 2007, 129, 14118-14119.	13.7	58
267	Solid-State NMR Spectroscopy of a Paramagnetic Protein: Assignment and Study of Human Dimeric Oxidized Cull–ZnII Superoxide Dismutase (SOD). Angewandte Chemie - International Edition, 2007, 46, 1079-1082.	13.8	100
268	On the orientational dependence of resolution in1H solid-state NMR, and its role in MAS, CRAMPS and delayed-acquisition experiments. Magnetic Resonance in Chemistry, 2007, 45, S93-S100.	1.9	15
269	Editorial. Magnetic Resonance in Chemistry, 2007, 45, S1-S1.	1.9	0
270	Fast adiabatic pulses for solid-state NMR of paramagnetic systems. Chemical Physics Letters, 2007, 435, 157-162.	2.6	112

#	Article	IF	CITATIONS
271	The influence of nitrogen-15 proton-driven spin diffusion on the measurement of nitrogen-15 longitudinal relaxation times. Journal of Magnetic Resonance, 2007, 184, 51-61.	2.1	57
272	The refocused INADEQUATE MAS NMR experiment in multiple spin-systems: Interpreting observed correlation peaks and optimising lineshapes. Journal of Magnetic Resonance, 2007, 188, 24-34.	2.1	76
273	The role of 15N CSA and CSA/dipole cross-correlation in 15N relaxation in solid proteins. Journal of Magnetic Resonance, 2007, 186, 26-33.	2.1	7
274	Assigning carbon-13 NMR spectra to crystal structures by the INADEQUATE pulse sequence and first principles computation: a case study of two forms of testosterone. Physical Chemistry Chemical Physics, 2006, 8, 137-143.	2.8	142
275	Accurate Measurements of13Câ~13CJ-Couplings in the Rhodopsin Chromophore by Double-Quantum Solid-State NMR Spectroscopy. Journal of the American Chemical Society, 2006, 128, 3878-3879.	13.7	38
276	Molecular Structure Determination in Powders by NMR Crystallography from Proton Spin Diffusion. Journal of the American Chemical Society, 2006, 128, 9555-9560.	13.7	165
277	Assigning powders to crystal structures by high-resolution1H–1H double quantum and1H–13C J-INEPT solid-state NMR spectroscopy and first principles computation. A case study of penicillin G. Physical Chemistry Chemical Physics, 2006, 8, 3418-3422.	2.8	79
278	Better Characterization of Surface Organometallic Catalysts through Resolution Enhancement in Proton Solid State NMR Spectra. Inorganic Chemistry, 2006, 45, 9587-9592.	4.0	25
279	Selective NMR Measurements of Homonuclear Scalar Couplings in Isotopically Enriched Solids. Journal of Physical Chemistry B, 2006, 110, 16982-16991.	2.6	48
280	Investigation of Dipolar-Mediated Waterâ^Protein Interactions in Microcrystalline Crh by Solid-State NMR Spectroscopy. Journal of the American Chemical Society, 2006, 128, 8246-8255.	13.7	69
281	Solid-State NMR of a Paramagnetic DIAD-FellCatalyst:Â Sensitivity, Resolution Enhancement, and Structure-Based Assignments. Journal of the American Chemical Society, 2006, 128, 13545-13552.	13.7	112
282	Observation of Heteronuclear Overhauser Effects Confirms the15Nâ^'1H Dipolar Relaxation Mechanism in a Crystalline Protein. Journal of the American Chemical Society, 2006, 128, 12398-12399.	13.7	36
283	Triple-quantum correlation NMR experiments in solids using J-couplings. Journal of Magnetic Resonance, 2006, 179, 49-57.	2.1	36
284	Floquet–van Vleck analysis of heteronuclear spin decoupling in solids: The effect of spinning and decoupling sidebands on the spectrum. Solid State Nuclear Magnetic Resonance, 2006, 29, 30-51.	2.3	16
285	Surface versus Molecular Siloxy Ligands in Well-Defined Olefin Metathesis Catalysts: [{(RO)3SiO}Mo(NAr)(CHtBu)(CH2tBu)]. Angewandte Chemie - International Edition, 2006, 45, 1216-122	20 <sup>13.8</sup>	155
286	Chemical Shift Correlations in Disordered Solids. Journal of the American Chemical Society, 2005, 127, 4466-4476.	13.7	71
287	Complete Assignment of Heteronuclear Protein Resonances by Protonless NMR Spectroscopy. Angewandte Chemie - International Edition, 2005, 44, 3089-3092.	13.8	162
288	Multi-dimensional magnetic resonance imaging in a stray magnetic field. Journal of Magnetic Resonance, 2005, 172, 79-84.	2.1	18

LYNDON EMSLEY

#	Article	IF	CITATIONS
289	Water–Protein Hydrogen Exchange in the Micro-Crystalline Protein Crh as Observed by Solid State NMR Spectroscopy. Journal of Biomolecular NMR, 2005, 32, 195-207.	2.8	50
290	Through-space contributions to two-dimensional double-quantum J correlation NMR spectra of magic-angle-spinning solids. Journal of Chemical Physics, 2005, 122, 194313.	3.0	82
291	Quantitative Analysis of Backbone Dynamics in a Crystalline Protein from Nitrogen-15 Spinâ`Lattice Relaxation. Journal of the American Chemical Society, 2005, 127, 18190-18201.	13.7	111
292	Powder Crystallography by Proton Solid-State NMR Spectroscopy. Journal of the American Chemical Society, 2005, 127, 9140-9146.	13.7	164
293	Well-Defined Surface Tungstenocarbyne Complexes through the Reaction of [W(â‹®CtBu)(CH2tBu)3] with Silica. Organometallics, 2005, 24, 4274-4279.	2.3	79
294	Proton to Carbon-13 INEPT in Solid-State NMR Spectroscopy. Journal of the American Chemical Society, 2005, 127, 17296-17302.	13.7	138
295	Characterization of heteronuclear decoupling through proton spin dynamics in solid-state nuclear magnetic resonance spectroscopy. Journal of Chemical Physics, 2004, 121, 3165-3180.	3.0	50
296	Probing Protonâ^'Proton Proximities in the Solid State:Â High-Resolution Two-Dimensional1Hâ^'1H Double-Quantum CRAMPS NMR Spectroscopy. Journal of the American Chemical Society, 2004, 126, 13230-13231.	13.7	118
297	Transverse Dephasing Optimised NMR Spectroscopy in Solids: Natural-Abundance13C Correlation Spectra. ChemPhysChem, 2004, 5, 869-875.	2.1	34
298	Principles of Spin-Echo Modulation byJ-Couplings in Magic-Angle-Spinning Solid-State NMR. ChemPhysChem, 2004, 5, 815-833.	2.1	84
299	The 2D MAS NMR spin-echo experiment: the determination of 13C–13C J couplings in a solid-state cellulose sample. Journal of Magnetic Resonance, 2004, 171, 43-47.	2.1	35
300	Direct spectral optimisation of proton–proton homonuclear dipolar decoupling in solid-state NMR. Chemical Physics Letters, 2004, 398, 532-538.	2.6	188
301	Site-Specific Backbone Dynamics from a Crystalline Protein by Solid-State NMR Spectroscopy. Journal of the American Chemical Society, 2004, 126, 11422-11423.	13.7	87
302	Molecular Understanding of the Formation of Surface Zirconium Hydrides upon Thermal Treatment under Hydrogen of [(â‹®SiO)Zr(CH2tBu)3] by Using Advanced Solid-State NMR Techniques. Journal of the American Chemical Society, 2004, 126, 12541-12550.	13.7	127
303	Detailed Structural Investigation of the Grafting of [Ta(CHtBu)(CH2tBu)3] and [Cp*TaMe4] on Silica Partially Dehydroxylated at 700 °C and the Activity of the Grafted Complexes toward Alkane Metathesis. Journal of the American Chemical Society, 2004, 126, 13391-13399.	13.7	136
304	Heteronuclear decoupling in NMR of Liquid Crystals using continuous phase modulation. Chemical Physics Letters, 2003, 368, 511-522.	2.6	42
305	Improved heteronuclear decoupling schemes for solid-state magic angle spinning NMR by direct spectral optimization. Chemical Physics Letters, 2003, 376, 259-267.	2.6	63
306	Correlation of fast and slow chemical shift spinning sideband patterns under fast magic-angle spinning. Journal of Magnetic Resonance, 2003, 160, 40-46.	2.1	27

#	Article	IF	CITATIONS
307	Carbon-13 lineshapes in solid-state NMR of labeled compounds. Effects of coherent CSA–dipolar cross-correlation. Journal of Magnetic Resonance, 2003, 162, 90-101.	2.1	34
308	Experimental aspects of proton NMR spectroscopy in solids using phase-modulated homonuclear dipolar decoupling. Journal of Magnetic Resonance, 2003, 163, 105-113.	2.1	169
309	Spin-state selection in solid-state NMR. Journal of Magnetic Resonance, 2003, 164, 187-195.	2.1	66
310	High-Resolution NMR Correlation Spectra of Disordered Solids. Journal of the American Chemical Society, 2003, 125, 4376-4380.	13.7	110
311	Resolution Enhancement in Multidimensional Solid-State NMR Spectroscopy of Proteins Using Spin-State Selection. Journal of the American Chemical Society, 2003, 125, 11816-11817.	13.7	66
312	Perhydrocarbyl ReVIIComplexes: Comparison of Molecular and Surface Complexes. Journal of the American Chemical Society, 2003, 125, 492-504.	13.7	116
313	The performance of phase modulated heteronuclear dipolar decoupling schemes in fast magic-angle-spinning nuclear magnetic resonance experiments. Journal of Chemical Physics, 2003, 119, 4833-4841.	3.0	72
314	The Direct Detection of a Hydrogen Bond in the Solid State by NMR through the Observation of a Hydrogen-Bond Mediated15Nâ~15NJCoupling. Journal of the American Chemical Society, 2002, 124, 1152-1153.	13.7	77
315	Through-bond phosphorus–phosphorus connectivities in crystalline and disordered phosphates by solid-state NMR. Chemical Communications, 2002, , 1702-1703.	4.1	66
316	A New NMR Method for the Study of Local Mobility in Solids and Application to Hydration of Biopolymers in Plant Cell Walls. Macromolecules, 2002, 35, 5078-5084.	4.8	27
317	Molecular Insight Into Surface Organometallic Chemistry Through the Combined Use of 2D HETCOR Solid-State NMR Spectroscopy and Silsesquioxane Analogues. Angewandte Chemie - International Edition, 2002, 41, 16-16.	13.8	1
318	Observation of a H-Agostic Bond in a Highly Active Rhenium–Alkylidene Olefin Metathesis Heterogeneous Catalyst by Two-Dimensional Solid-State NMR Spectroscopy. Angewandte Chemie - International Edition, 2002, 41, 4535-4538.	13.8	77
319	Sample Restriction Using Radiofrequency Field Selective Pulses in High-Resolution Solid-State NMR. Journal of Magnetic Resonance, 2002, 154, 136-141.	2.1	19
320	Improved Resolution in Proton NMR Spectroscopy of Powdered Solids. Journal of the American Chemical Society, 2001, 123, 5747-5752.	13.7	71
321	Protonâ <sup>~^</sup> Proton Constraints in Powdered Solids from1Hâ <sup>~^</sup> 1Hâ <sup>~^</sup> 1H and1Hâ <sup>~^</sup> 1Hâ <sup>~^</sup> 13C Three-Dimensional NMR Chemical Shift Correlation Spectroscopy. Journal of the American Chemical Society, 2001, 123, 5604-5605.	13.7	27
322	Characterization of Surface Organometallic Complexes Using High Resolution 2D Solid-State NMR Spectroscopy. Application to the Full Characterization of a Silica Supported Metal Carbyne: â‹®SiOâ''Mo(â‹®Câ^'Bu-t)(CH2â^'Bu-t)2. Journal of the American Chemical Society, 2001, 123, 3820-3821.	13.7	72
323	Segmental mobility in poly(isoprene) rubber studied by deuterium-carbon NMR correlation spectroscopy. Polymer Bulletin, 2001, 46, 183-190.	3.3	4
324	Through-Bond Heteronuclear Single-Quantum Correlation Spectroscopy in Solid-State NMR, and Comparison to Other Through-Bond and Through-Space Experiments. Journal of Magnetic Resonance, 2001, 148, 449-454.	2.1	99

#	Article	IF	CITATIONS
325	Spectral Editing in Solid-State NMR Using Scalar Multiple Quantum Filters. Journal of Magnetic Resonance, 2001, 151, 40-47.	2.1	43
326	Synthesis of Deuterium-Labeled Cryptophane-A and Investigation of Xe@Cryptophane Complexation Dynamics by 1D-EXSY NMR Experiments. Chemistry - A European Journal, 2001, 7, 1561-1573.	3.3	74
327	Solid-State NMR Spectroscopy and Silsesquioxane Analógues We are also indebted to the CNRS, ENS Lyon, and ESCPE Lyon for financial support. M.C. is grateful to the French ministry of education, research, and technology (MENRT) for a pre-doctoral fellowship. E.A.Q. gratefully acknowledges Università di Pisa and S.N.A.M. for financial support. 2D HETCOR=two-dimensional heteronuclear	13.8	76
328	correlation Angewandte Chemie - International Edition, 2001, 40, 4493. Sample Restriction Using Magnetic Field Gradients in High-Resolution Solid-State NMR. Journal of Magnetic Resonance, 2000, 145, 334-339.	2.1	19
329	Simulation of extended periodic systems of nuclear spins. Chemical Physics Letters, 2000, 326, 515-522.	2.6	32
330	Homonuclear dipolar decoupling in solid-state NMR using continuous phase modulation. Chemical Physics Letters, 2000, 319, 253-260.	2.6	282
331	Sensitivity enhancement of the central transition NMR signal of quadrupolar nuclei under magic-angle spinning. Chemical Physics Letters, 2000, 327, 85-90.	2.6	204
332	Carbon-13 Solid-State NMR Studies on Synthetic Model Compounds of [4Feâ^'4S] Clusters in the 2+ State. Journal of Physical Chemistry A, 2000, 104, 9990-10000.	2.5	31
333	129Xe NMR Spectroscopy of Deuterium-Labeled Cryptophane-A Xenon Complexes:Â Investigation of Hostâ^'Guest Complexation Dynamics. Journal of the American Chemical Society, 2000, 122, 1171-1174.	13.7	95
334	Complete Resonance Assignment of a Natural Abundance Solid Peptide by Through-Bond Heteronuclear Correlation Solid-State NMR. Journal of the American Chemical Society, 2000, 122, 9739-9744.	13.7	73
335	Solid-state NMR characterization of hydration effects on polymer mobility in onion cell-wall material. Carbohydrate Research, 1999, 322, 102-112.	2.3	57
336	Experimental observation of periodic quasi-equilibria in solid-state NMR. Chemical Physics Letters, 1999, 308, 381-389.	2.6	30
337	The Accuracy of Distance Measurements in Solid-State NMR. Journal of Magnetic Resonance, 1999, 139, 46-59.	2.1	67
338	Through-Bond Carbonâ^'Carbon Connectivities in Disordered Solids by NMR. Journal of the American Chemical Society, 1999, 121, 10987-10993.	13.7	412
339	Quasi equilibria in solid-state NMR. Chemical Physics Letters, 1998, 293, 110-118.	2.6	20
340	Intrinsic Asymmetry in Multidimensional Solid-State NMR Correlation Spectra. Journal of Magnetic Resonance, 1998, 130, 233-237.	2.1	11
341	Assignment and Measurement of Deuterium Quadrupolar Couplings in Liquid Crystals by Deuteriumâ^'Carbon NMR Correlation Spectroscopy. Journal of Physical Chemistry B, 1998, 102, 3718-3723.	2.6	28
342	Carbonâ^'Proton Chemical Shift Correlation in Solid-State NMR by Through-Bond Multiple-Quantum Spectroscopy. Journal of the American Chemical Society, 1998, 120, 13194-13201.	13.7	206

#	Article	IF	CITATIONS
343	Carbon-13 Spectral Editing in Solid-State NMR Using Heteronuclear Scalar Couplings. Journal of the American Chemical Society, 1998, 120, 7095-7100.	13.7	86
344	Solution-State NMR Studies of the Surface Structure and Dynamics of Semiconductor Nanocrystals. Journal of Physical Chemistry B, 1998, 102, 10117-10128.	2.6	67
345	Deuterium to carbon cross-polarization in liquid crystals. Journal of Chemical Physics, 1998, 109, 1873-1884.	3.0	21
346	Unidirectional Steady State Rates of Central Metabolism Enzymes Measured Simultaneously in a Living Plant Tissue. Journal of Biological Chemistry, 1998, 273, 25053-25061.	3.4	41
347	Determination of Through-Bond Carbonâ^ Carbon Connectivities in Solid-State NMR Using the INADEQUATE Experiment. Journal of the American Chemical Society, 1997, 119, 7867-7868.	13.7	210
348	Deuteriumâ^'Carbon NMR Correlation Spectroscopy in Oriented Materials. Journal of the American Chemical Society, 1997, 119, 12000-12001.	13.7	22
349	The reliability of the determination of tensor parameters by solid-state nuclear magnetic resonance. Journal of Chemical Physics, 1997, 107, 4808-4816.	3.0	106
350	Two-dimensional spin-exchange solid-state NMR studies of 13C-enriched wood. Solid State Nuclear Magnetic Resonance, 1997, 8, 25-32.	2.3	75
351	Long-Range Dipolar Couplings in Liquid Crystals Measured by Three-Dimensional NMR Spectroscopy. Journal of the American Chemical Society, 1996, 118, 12224-12225.	13.7	24
352	Improved Sensitivity in Selective NMR Correlation Spectroscopy and Applications to the Determination of Scalar Couplings in Peptides and Proteins. Journal of the American Chemical Society, 1996, 118, 9320-9325.	13.7	2
353	The Effect of Imperfect Saturation in Saturation-RecoveryT1Measurements. Journal of Magnetic Resonance Series A, 1996, 118, 108-112.	1.6	13
354	The effect of spin decoupling on line shapes in solidâ€ <b>s</b> tate nuclear magnetic resonance. Journal of Chemical Physics, 1996, 104, 2518-2528.	3.0	29
355	Measurement of Carbonâ^Proton Dipolar Couplings in Liquid Crystals by Local Dipolar Field NMR Spectroscopy. The Journal of Physical Chemistry, 1996, 100, 18696-18701.	2.9	85
356	[5] Selective pulses and their applications to assignment and structure determination in nuclear magnetic resonance. Methods in Enzymology, 1994, 239, 207-246.	1.0	32
357	Methods for reconstructing phase sensitive slice profiles in magnetic resonance imaging. Magnetic Resonance in Medicine, 1994, 31, 178-183.	3.0	7
358	Determination of DNA conformational features from selective two-dimensional NMR experiments. Journal of the American Chemical Society, 1993, 115, 7765-7771.	13.7	18
359	Optimization of shaped selective pulses for NMR using a quaternion description of their overall propagators. Journal of Magnetic Resonance, 1992, 97, 135-148.	0.5	102
360	NMR studies of the surface structure and dynamics of semiconductor nanocrystals. Chemical Physics Letters, 1992, 198, 431-436.	2.6	109

#	Article	IF	CITATIONS
361	NMR studies of an oligoproline-containing peptide analog that binds specifically to the H-2Kd histocompatibility molecule. Biochemistry, 1991, 30, 9429-9434.	2.5	8
362	Selective two-dimensional NMR experiments for topological filtration of fragments of coupling networks. Journal of the American Chemical Society, 1991, 113, 3309-3316.	13.7	21
363	On the use of a slice-selective 270° self-refocusing Gaussian pulse for magnetic resonance imaging: Comments on the note by D. M. Doddrellet al Magnetic Resonance in Medicine, 1991, 19, 461-463.	3.0	3
364	The Role of Selective Two-Dimensional NMR Correlation Methods in Supplementing Computer-Supported Multiplet Analysis by MARCO POLO. , 1991, , 151-162.		0
365	Phase shifts induced by transient Bloch-Siegert effects in NMR. Chemical Physics Letters, 1990, 168, 297-303.	2.6	77
366	Gaussian pulse cascades: New analytical functions for rectangular selective inversion and in-phase excitation in NMR. Chemical Physics Letters, 1990, 165, 469-476.	2.6	323
367	Unraveling Overlapping Multiplets in Two-Dimensional NMR Correlation Spectra by Selective Inversion of Coupling Partners. Angewandte Chemie International Edition in English, 1990, 29, 517-520.	4.4	25
368	Entflechtung überlagernder Multipletts in zweidimensionalen NMRâ€Korrelationsspektren durch selektive Inversion der Spins der Kopplungspartner. Angewandte Chemie, 1990, 102, 576-579.	2.0	6
369	Volume-selective NMR spectroscopy with self-refocusing pulses. Journal of Magnetic Resonance, 1990, 87, 1-17.	0.5	7
370	Double selective inversion in NMR and multiple quantum effects in coupled spin systems. Journal of Magnetic Resonance, 1990, 90, 214-220.	0.5	20
371	Gaussian Pulse Cascades and Selective Two-Dimensional NMR. , 1990, , 449-450.		0
372	Self-refocusing effect of 270° Gaussian pulses. Applications to selective two-dimensional exchange spectroscopy. Journal of Magnetic Resonance, 1989, 82, 211-221.	0.5	68
373	Self-refocusing 270° gaussian pulses for slice selection without gradient reversal in magnetic resonance imaging. Magnetic Resonance in Medicine, 1989, 10, 273-281.	3.0	17
374	Longitudinal relaxation pathways in scalar-coupled systems. Journal of Magnetic Resonance, 1989, 81, 13-42.	0.5	11